Research Square

Preprints are preliminary reports that have not undergone peer review.
They should not be considered conclusive, used to inform clinical practice,
or referenced by the media as validated information.

Nano calcium phosphate improves growth and reduces arsenic in rice

Kavita Shukla
Banaras Hindu University
Shiwanshu Shekhar
Matsui Engineering Private Limited
Nidhi Tyagi
Banaras Hindu University
Rubina Khanam
ICAR- National Rice Research Institute
Jayanta kumar Biswas
University of Kalyani
Sudhakar Srivastava
sudhakar.iesd@bhu.ac.in
Banaras Hindu University
Shraddha Singh
Bhabha Atomic Research Centre

Research Article

Keywords: Hydroxyapatites nanoparticles (HANPs), physicochemical evaluation, sustainability

Posted Date: June 9th, 2026

DOI: https://doi.org/10.21203/rs.3.rs-9073474/v1

License: This work is licensed under a Creative Commons Attribution 4.0 International License.
Read Full License

Additional Declarations: No competing interests reported.

Nano calcium phosphate improves growth and reduces arsenic in rice

[1]Kavita Shukla, [2]Shiwanshu Shekhar, [3]Nidhi Tyagi, [4]Rubina Khanam, [5]Jayanta Kumar Biswas, [1]*Sudhakar Srivastava, [6] * Shraddha Singh

[1]Plant Stress Biology Laboratory, Institute of Environment & Sustainable Development (IESD), Banaras Hindu University (BHU), Varanasi, Uttar Pradesh-221005, India

[2]Matsui Engineering Private Limited, Ranchi, India

[3]Plant Stress Biology Laboratory, Institute of Environment & Sustainable Development (IESD), Banaras Hindu University (BHU), Varanasi, Uttar Pradesh-221005, India

[4]ICAR- National Rice Research Institute, Cuttack-753006, Odisha, India

[5]Enviromicrobiology, Ecotoxicology & Ecotechnology Laboratory (3E-MicroToxTech Lab), Department of Ecological Studies & International Centre for Ecological Engineering, University of Kalyani, Kalyani, Nadia- 741235, West Bengal, India

[6] Nuclear Agriculture & Biotechnology Division, Bhabha Atomic Research Centre, Trombay, Mumbai 400085, Maharashtra, India

*Correspondence to: Dr. Sudhakar Srivastava, Assistant Professor, Dr. Shraddha Singh, Scientific Officer 'F'

E-mail: sudhakar.iesd@bhu.ac.in, Shradhas@barc.gov.in

Abstract:

Background

Phosphorus (P) deficiency is a major constraint to rice productivity, particularly in arsenic (As)-contaminated soils where nutrient availability and uptake are severely impaired. The interaction between arsenic and phosphorus further aggravates toxicity and limits crop performance. This study evaluated the effectiveness of composite nanocalcium phosphate (NCaP) and hydroxyapatite nanoparticles (HANPs; particle size 15–45 nm, Ca/P ratio 1.7) as sustainable alternatives to conventional diammonium phosphate (DAP) fertilizer for rice cultivation in As-contaminated agricultural fields of Ghazipur and Jaunpur, Uttar Pradesh.

Results

Application of NCaP significantly enhanced rice growth and yield attributes compared with both DAP and control treatments. Panicle length increased by 1.8–4.5%, the number of grains per panicle by 4.9–6.6%, fertile spikelet counts by 4.9–8.4%, and 1000-grain weight by 10.6–28%, indicating substantial yield improvement. NCaP treatments also improved plant physiological health, as evidenced by reduced electrolyte leakage and lipid peroxidation, along with enhanced pigment content, reflecting improved membrane integrity and photosynthetic capacity.

Oxidative stress was markedly alleviated in NCaP-treated plants, with malondialdehyde (MDA) levels in shoots reduced by 21–30%. Activities of key antioxidant enzymes, including ascorbate peroxidase (APX), guaiacol peroxidase (GPX), superoxide dismutase (SOD), and catalase (CAT), were favorably modulated, indicating enhanced stress tolerance. Importantly, NCaP application significantly reduced As accumulation in rice grains while simultaneously improving P uptake in roots, shoots, and grains, with the highest P concentration (23 mg g^{-1}) recorded in T2-treated plants.

Conclusion

The findings demonstrate that NCaP nanoparticles can effectively replace conventional DAP fertilizer by improving nutrient use efficiency, enhancing crop growth and yield, strengthening physiological resilience, and mitigating arsenic accumulation in rice grains. These results highlight the promising role of nanotechnology-based fertilizers in promoting sustainable agriculture and ensuring food safety in arsenic-affected regions**.**

Keywords: Hydroxyapatites nanoparticles (HANPs), physicochemical evaluation, sustainability

Introduction:

Phosphorus (P) ranks as the second most crucial element following nitrogen (N) due to its significant impact on both aquatic and terrestrial ecosystems' productivity and vitality. It is a fundamental element for achieving optimal crop productivity on arable lands worldwide [1].The insufficiency of phosphorus acts as a significant abiotic stressor impacting global plant growth and crop yield[2]. The accumulation of anthocyanin in plants serves as a visible indicator of inorganic phosphate (Pi) deficiency, leading to the purpling of leaves, stems, and, at times, roots[38]. The presence of Pi in soil is often limited as it readily binds to soil particles. In calcareous-to-neutral soils, Pi can precipitate with calcium (Ca^{2+}), forming a plant-accessible

dicalcium phosphate form. However, this compound can further convert into more stable forms such as hydroxyapatite and octocalcium phosphate, resulting in reduced plant accessibility, especially in alkaline soil pH conditions [3].

The use of phosphorus (P) fertilizers to augment crop productivity is widespread. Nevertheless, further advancements in analytical and theoretical methodologies are imperative for a comprehensive understanding and management of the soil P cycle. Many soils inherently possess low P accessibility, despite having a significant total P quantity [4]. Excessive use of P fertilizers to enhance plant availability contributes to the problem of eutrophication in surface waters. Consequently, various regulations and best management practices aim to curtail the entry of P into water bodies.

The primary food source for the residents of the arsenic-impacted areas of India's Gangetic plains is rice, which is grown extensively there. Among crop plants, rice is thought to be the most promising accumulator of As [5,6]. Arsenic buildup in rice grains is an emerging issue that requires the application of viable, sustainable, and effective strategies [6]. Arsenic and P share similarities in their uptake by rice plants. Both elements are absorbed by the plant's roots, often using similar transport pathways, leading to potential competition for uptake [7]. This can result in reduced P uptake in the presence of high As levels due to the shared transport systems. However, P is an essential nutrient for plant growth, while As is toxic. This highlights the importance of ensuring an adequate supply of P to promote healthy rice growth while minimizing the uptake of harmful As. Balancing P and As uptake is crucial in rice cultivation to ensure both nutrient sufficiency and food safety.

Nanoparticles have gained attention in the context of mitigating metal contamination in agricultural systems [8]. These nanoparticles, often engineered at the nanoscale, offer a novel approach to address the co-occurrence of phosphorus deficiency and metal(loid) toxicity in rice fields. One of the key strategies involves designing P nanoparticles to enhance P availability for rice plants while minimizing the uptake of toxic As. These nanoparticles can be used to optimize the delivery of P to plant roots, promoting healthier crop growth. By using traditional techniques like spraying or irrigation, P nanoparticles can readily enter the root zone [9] As opposed to its soluble forms, P in solid form has significantly less bioavailability to algae, making these nanoparticles environmentally benign [10]. Simultaneously, they act as a barrier, reducing the absorption of toxic metal(loid) by plant roots, thus minimizing the transfer of this toxic element into the edible parts of the rice plant [11].

Recognizing the vital role of fertilizers, the emergence of nano-based fertilizers presents a novel technological avenue in agriculture. These nano-fertilizers, aiming for a high surface area-to-volume ratio by minimizing bulk materials to less than 100 nm, are more soluble and reactive compared to their conventional counterparts [12]. This research investigates the effects of synthesized nano-calcium phosphate (NCaP) through foliar and soil applications on rice crops compared to conventional diammonium phosphate (DAP) fertilizer. The study focuses on assessing their impact on yield and As uptake in rice crops. This innovative approach holds promise in ensuring food safety and security, particularly in regions with As contaminated soils. By harnessing the unique properties of phosphorus nanoparticles, we aim to address the complex challenge of managing nutrient deficiencies and toxic element As accumulation in crops like rice.

Material and methods:

2.1 Nanoparticle synthesis and characterization:

In this research, all compounds used were of a high level of purity, meeting either analytical-grade or higher standards. These chemicals were procured from Hi-media, a reputable source. The water utilized for the preparation of each solution was deionized (DI), ensuring its purity.

The synthesis of composite phosphorus nanoparticles followed the methodology established by [13]. Specific solutions containing Carboxymethyl cellulose (CMC), phosphate ions (PO_4^{3-}), and calcium ions (Ca^{2+}) were prepared using NaCMC, H_3PO_4, and $Ca(OH)_2$, respectively. The synthesis of composite nano-calcium phosphate (NCaP) was conducted in a standard laboratory environment. Initially, a 50 ml CMC solution was prepared and subjected to continuous stirring on a magnetic stirrer. Subsequently, 25 ml of Ca^{2+} solution was added drop wise to this CMC solution. Following 12 hours of continuous stirring, 25 ml of the H_3PO_4 solution was introduced drop wise into the stirring mixture. The resulting precipitate was allowed to settle, and the supernatant was decanted. The remaining precipitate was subjected to filtration and washed thrice with distilled water. Finally, the solid obtained was dried using a freeze drier overnight.

The synthesis of phosphorus fertilizer without CMC was conducted following a similar procedure, except for the exclusion of NaCMC. In this process, 200 ml of H_3PO_4 (0.6 mol L^{-1} was added drop wise to 200 ml of $Ca(OH)_2$ (1 mol L^{-1}) under mechanical stirring (300 rpm) for 3 hrs. Then the suspension was kept in rest for 2 hrs, filtered to remove as much of the

aqueous medium as possible and freeze dried. The remaining steps were identical to the composite hydroxynanoparticle synthesis.

Characterization of the synthesized nanoparticles involved several analytical techniques, including Fourier Transform Infrared (FTIR) Spectroscopy using the Thermo Electron Scientific Instruments LLC's Nicolet iS5 instrument. X-ray Diffraction (XRD) analysis was carried out with the Rigaku SmartLab 9 kW Powder-type instrument. Scanning Electron Microscopy (SEM) analysis was performed utilizing the Carl Zeiss EVO-18, a research model from Germany. Dynamic Light Scattering (DLS) and Zeta potential analysis were conducted with the Zetasizer Nano ZS90, manufactured by Malvern.

These techniques were instrumental in characterizing the synthesized product. FTIR spectroscopy played a crucial role in identifying the functional groups associated with the composite hydroxynanoparticles. XRD analysis was employed to determine the crystal d-spacing of the nano-powder. SEM-EDX analysis facilitated the examination of morphology and the weight percentage of elements present in the nano-powder.

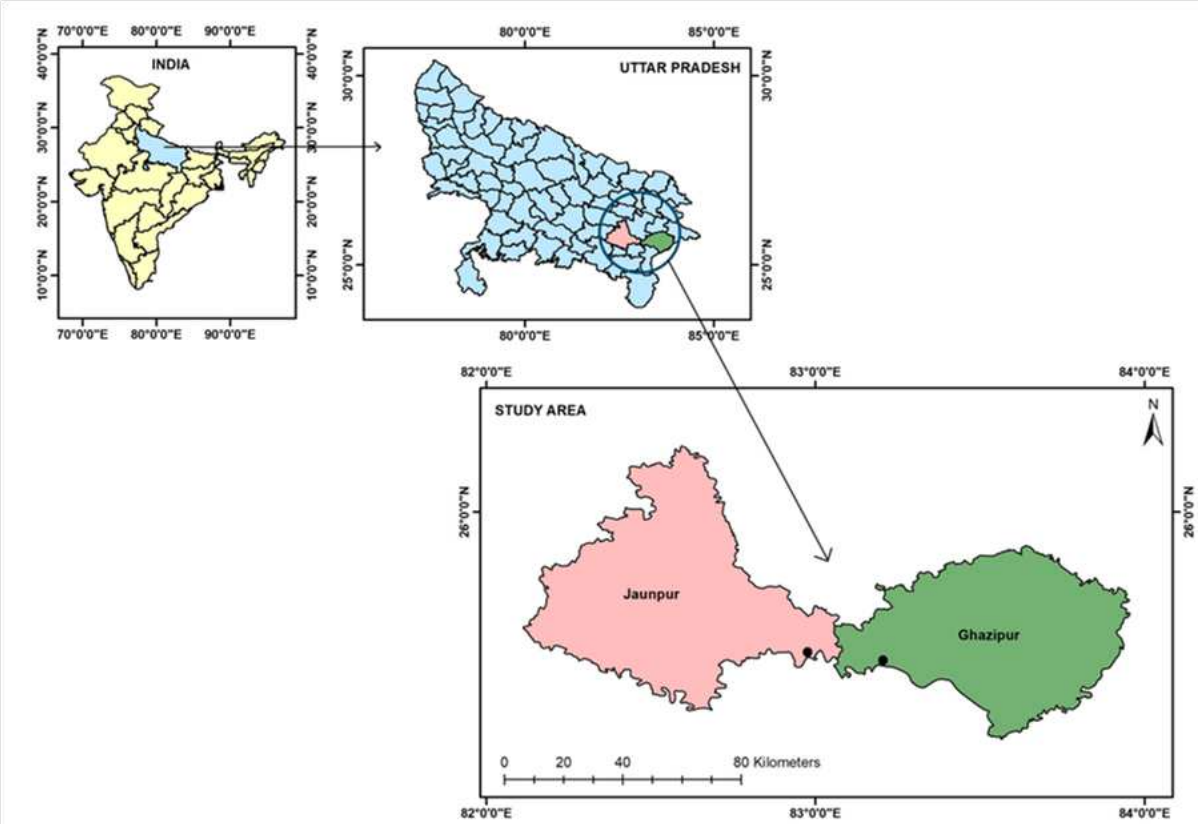
2.2 Study area

In the study, arsenic-contaminated fields in two distinct areas, Ghazipur and Jaunpur in Uttar Pradesh, were selected to investigate the impact of nanophosphorus on specific rice varieties. Positioned at coordinates 25°32'51.3"N 83°13'36.8"E for Saidpur, Ghazipur and 25°34'22.1"N 82°58'32.0" E for Bhainsa, Jaunpurr, these fields were chosen due to their similar contamination levels. The experimental setup encompassed a 900 cm^2 area, structured in a three-replicate randomized complete block design (RCBD). Two rice genotypes were selected from our previous hydroponic study based on their phosphorus use efficiency (PUE) and response to phosphorus availability[49]. The genotype DS (DNA Sribala, maturation time: 135 days), which exhibited the highest PUE and strong responsiveness to phosphorus, and SK (Sai Kasturi, maturation time: 125 days), which showed the lowest PUE and poor phosphorus response, were chosen for the field study. Treatments included a control with standard diammonium phosphate (DAP) fertilization, foliar NCaP (nano-calcium phosphate) application (T1) 20 mg L^{-1}, and composite NCaP (composite nano-calcium phosphate) mixed into the soil at 30 mg kg^{-1} (T2) for the both varieties. Our initial pot studies with three concentrations of NCaP (20, 30, 60 mg kg^{-1})/ mg L^{-1} served as the basis for the dosage of NCaP that was selected. Control block, phosphorus was supplied via DAP (as part of NPK), whereas in the treated block, phosphorus was supplied solely through nano-hydroxyapatite, with

158 nitrogen and potassium inputs balanced to maintain parity with the control. After analyzing the
159 morphological changes, phenotypic appearance, physiological response, and phosphorus
160 content of thirty-day-old rice seedlings, it was shown that 30 mg kg^{-1} (soil applied) or 20 mg
161 L^{-1} (foliar application) produced the greatest outcomes.

162 For T2, soil composite NCaP was infused at a 20 cm depth, with an extraction of 49.5 kg of
163 soil taken from a 900 cm^2 area. Subsequently, 1.5 g of total composite NCaP (20mg kg^{-1}) was
164 added to the extracted soil from 900 cm^2 area. The foliar application of NCaP through spraying
165 was performed thrice with 0.1% (v/v) Tween 20 (0.1ml in 1L solution), at different stages, i.e.,
166 15, 45, and 65 days after transplanting using a hand-held sprayer. To improve foliar sprayed
167 NPs' absorption, Tween-20 was used as a surfactant Liu *et al* [13]. A solution comprising NCaP
168 sonicated in high quality ultrapure water (Milli-Q) for 30 minutes was adjusted to a total
169 volume of 1 L as required. During the application phases, the initial spray necessitated 300 ml
170 for one block. At 45 days, 700 ml was needed, and by 65 days, only 1L was necessary. The
171 concentration of the NCaP solution was maintained at 30 mg L^{-1}. In the control block, NPK
172 was treated at 40–60–120 kg correspondingly according to local farmers' practices. While NK
173 was the only fertilizer administered in the treated block at the same ratio P was replaced by
174 Nano hydroxyapetite fertilizer. In two stages during field preparation and the tillering stage
175 (between 35 and 45 days after planting) nitrogen and phosphate fertilizer, represented by urea
176 and DAP, respectively, were applied.

177



178

179 **Figure 1**: The map represents the selected contaminated field sites for the experiment

180

181 ***2.3 Soil Sampling and Physicochemical Analysis***

182 The soil sampling process involved two distinct phases initial sampling prior to transplantation
183 and a second phase time of harvesting. Soil samples, collected from the ploughing zone at a
184 depth of 0-20 cm, underwent various preparatory steps. After air drying, the soil was crushed,
185 sieved using a 2.0 mm sieve, and homogenized to facilitate physicochemical and As analyses.

186 The Olsen method was employed to assess available phosphorus content. This approach
187 entailed blending 2.5 grams of dry soil with charcoal and Olsen reagents. After filtration,
188 ammonium molybdate and $SnCl_2$ were incorporated into the mixture. At 660 nm, the intensity
189 of the blue color that resulted was measured. Determination of organic matter employed the [14]
190 method, using chemicals and titration with ferrous ammonium sulfate. Additionally, pH and
191 electrical conductivity (EC), ORP were measured at a 1:10 soil-to-water ratio using a
192 waterproof Oaklon multi-parameter tester (TCSTestrTM-35 series). Phosphomonoesterase
193 activity in soil can be estimated using the method of Tabatabai and Bremner (1969), which
194 involves the hydrolysis of p-nitrophenyl phosphate (pNPP) to p-nitrophenol (pNP). For acid

phosphatase, soil is incubated with pNPP in modified universal buffer (MUB) at pH 6.5; for alkaline phosphatase, the buffer is adjusted to pH 11.0. Approximately 1 g of soil is treated with 0.2 mL toluene, 4 mL of buffer, and 1 mL of pNPP solution, then incubated at 37 °C for 1 hour. The reaction is stopped with 1 mL 0.5 M $CaCl_2$ and 4 mL 0.5 M NaOH, which also develops the yellow color of pNP. The mixture is filtered, and absorbance is measured at 405 nm. Enzyme activity is expressed as µg pNP released per g soil per hour using a standard curve[15]. Soil (typically 1 g, moist or field-moist) is incubated with a protein substrate (e.g. casein) or a dipeptide derivative in a suitable buffer (e.g. Tris, pH ~8.0) under controlled temperature (often ~40–50 °C) for a short period (e.g. 1–2 h). After incubation, the reaction is terminated by adding cold trichloroacetic acid (TCA) to precipitate unhydrolyzed protein. The mixture is filtered or centrifuged, and the soluble hydrolysate (peptides, amino acids) is reacted with Folin–Ciocalteu reagent after suitable neutralization (e.g. with Na_2CO_3). The colored product (mostly from tyrosine/phenolic-amino acid residues) is measured spectrophotometrically (around 680 nm). The amount of released tyrosine equivalent (from calibration curve) is used to calculate protease (proteolytic) activity, typically expressed as mg tyrosine (or protein hydrolysate) per g soil per hour [16].

2.4 Harvesting, Growth, and Yield Measurement

Sampling was conducted twice during the growth cycle – first at 85 ds post-transplantation and then at maturity (135/120 DAT). Root and shoot lengths were measured using manual metric scales, and biomass data were recorded using a digital balance. Leaf samples were gathered for chlorophyll analysis and other biochemical tests. The final sampling at maturity included detailed estimations of plant yield, biomass, spikelet numbers, spikelet length, grain quality, and 1000 grain weight.

2.5 Sample Preparation for Groundwater and Soil Elemental Analysis

With the aid of a PVC core, soil samples (upper 20 cm) were obtained, dried in an oven at 60°C, and ground to less than 0.2 mm. Wavelength Dispersive X-ray Fluorescence (WD-XRF) (S8 TIGER, Bruker, Mannheim, Germany) was utilized for elemental analysis. Press pellet method were used to prepare the sample. Groundwater samples were obtained from shallow tube wells, and during the sampling process, the samples were field-treated with a few drops of 2% HNO_3 and then digested with 5N HNO_3 (5:50 V/V) at block digester then subjected to HG-AAS analysis.

2.6 Estimation of Arsenic and Phosphate Concentration in plant tissue and grain

Plant samples were divided into distinct components (root, flag leaves, and grains) and cleaned by gentle shaking, followed by drying in an oven. Once dried, grain samples were dehusked and crushed into powdered form. The samples underwent digestion with HNO_3 (70% Suprapur Merck; Darmstadt, Germany) using a heated test tube block digester at 180°C for one hour and later at 200°C for 45-60 minutes until the sample achieved a white crystalline form. Following digestion, the samples were adjusted to a final volume of 10 ml using ultrapure water (Type I), filtered through a 0.22 µm pore size filter paper, and assessed for As and phosphate concentrations via Hydride generation atomic absorption spectrophotometry (HG-AAS). For the hydride generation process, analytical grade sodium borohydride (3%; Merck), sodium hydroxide (2.5%; Merck), and hydrochloric acid (6 M; Merck) were utilized. The precision of the analysis was validated using certified standard reference materials (SRMs) from NIST, USA, specifically 1568a rice flour and 1573a tomato leaf, as detailed in [17]. The certified As concentrations for these materials are provided in Supplementary Table S1. Quality control was conducted through triplicate analyses and the measurement of recovery rates for spiked digested samples, with recoveries ranging from 95% to 98% for all tested samples.

2.7 Estimation of Pigment, Membrane Damage, and Electrolyte Leakage

Leaf tissue (or isolated chloroplasts) is homogenized in 80% acetone (v/v) and centrifuged to obtain a clear extract. The absorbances of the acetone extract are measured spectrophotometrically at 663 nm (A_{663}) and 645 nm (A_{645}). Chlorophyll concentrations are calculated using the following equations:

Chlorophyll a: $C_a = 12.7 \times A_{663} - 2.69 \times A_{645}$ (µg chlorophyll a per mL of extract)

Chlorophyll b: $Cb = 22.9 \times A_{645} - 4.68 \times A_{663}$ (µg chlorophyll b per mL)

Total chlorophyll (a + b): $C_{a+}b = 20.2 \times A_{645} + 8.02 \times A_{663}$ (µg/mL)

Then, using the volume of extract and the fresh weight of tissue, one converts these to µg (or mg) chlorophyll per g fresh weight[18,19]. Specific methods were employed to measure malondialdehyde (MDA), In which, Isolated chloroplasts are illuminated in an osmotic buffer medium, triggering photooxidative peroxidation of unsaturated lipids, which yields malondialdehyde (MDA). The reaction is followed kinetically: after illumination, the chloroplast suspension is acidified, and MDA is measured (usually via a thiobarbituric acid (TBA) reaction). The absorbance of the TBA–MDA complex (typically at ~532 nm, with correction at 600 nm) is used to quantify MDA. The rate of MDA formation under light versus

dark, and its stoichiometric relation with O_2 consumption and bleaching of chlorophyll, are used to interpret the kinetics and efficiency of photoperoxidation[19,20].For electrolyte leakage (EL),leaf discs (or segments) of uniform size are rinsed with deionized water to remove surface ions, then placed in a known volume of deionized water (e.g. 10–20 mL) and incubated (often 24 h at room temperature) with gentle shaking. The initial electrical conductivity (C_1) of the bathing solution is measured using a conductivity meter. Then the samples are boiled (or autoclaved) for ~10–15 min to fully release electrolytes, cooled, and the final conductivity (C_2) measured. Electrolyte leakage is calculated as:

$$\text{Electrolyte leakage } (\%) = C1/C2 \times 100$$

As described by [21]

2.8 Antioxidant enzyme assay

For antioxidant enzyme activity determination, 0.5 g of shoots and roots were homogenized in a 1.5 mL extraction buffer. The protein content was assessed using Bradford's method [22]. Superoxide dismutase (SOD) activity was evaluated using [23], which involved monitoring the suppression of photochemical reduction of nitro blue tetrazolium (NBT). 1 mL cold 100 mM K-phosphate buffer (pH 7.8) containing 0.1 mM ethylenediaminetetraacetic acid (EDTA), 1% (w/v) polyvinylpyrrolidone, and 0.5 percent (v/v) polyvinylpyrrolidone was used to homogenize the samples. The amount of enzyme required to cause 50% inhibition of NBT decrease as measured at 560 nm was defined as one unit of SOD activity. The rate of ascorbate oxidation was estimated to determine the activity of Ascorbate peroxidase (APX; extinction coefficient 2.8 mM^{-1} cm^{-1}). 50 mM phosphate buffer (pH 7.0), 0.1 mM H_2O_2, 0.5 mM sodium ascorbate, 0.1 mM EDTA, and a sufficient volume of enzyme extract were included in the 1 ml reaction mixture. At 290 nm, the change in absorbance was measured [23], and enzyme activity was measured in units of mg^{-1} protein. The activity of Glutathione peroxidase (GPX) was measured using the [24] 10 mL of 1% guaiacol (v/v), 10 mL of 0.3% H_2O_2, and 80 mL of 50 mM phosphate buffer were used in a 100 mL reaction mixture (pH 6.6). In a final amount of 1 mL, a suitable quantity of enzyme (25 µl) was added to the reaction mixture. At 470 nm, the increase in absorbance due to guaiacol oxidation (extinction coefficient 2.8 $mM^{-1}cm^{-1}$) was observed. Activity of Catalase (CAT) enzyme was estimated by the method given by [25] .50 mM sodium phosphate buffer (pH 7.0), 20 mM H_2O_2, and an appropriate amount of enzyme extract made up the 1 mL reaction mixture. At 240 nm, the decrease in absorbance owing to H_2O_2 consumption was observed (extinction coefficient 39.4 mM^{-1} cm^{-1})

2.9 Statistical Analysis

The experiment was conducted with three replications following a Randomized Complete Block Design (RCBD). Statistical analysis was performed using two-way analysis of variance (two-way ANOVA) in GraphPad Prism to evaluate the main effects of the experimental factors and their interaction. When significant effects were detected, mean comparisons were performed using Tukey's multiple comparison post hoc test. Differences were considered statistically significant at $p \leq 0.05$.

2.10. Quality control/assurance and instrument specification

The generation of hydride involved the utilization of analytical-grade sodium borohydride (3%; Merck), sodium hydroxide (2.5%; Merck), and hydrochloric acid (6 M; Merck). The accuracy of the analysis was verified using certified standard reference materials (SRMs) (NIST, USA), specifically 1568a rice flour and 1573a tomato leaf, following the protocols outlined in Khan et al. [26]. The certified As concentrations for 1568a rice flour and 1573a tomato leaf can be found in Supplementary Table S1. Quality control procedures comprised triple analyses and the determination of recovery from spiked digested samples, demonstrating recoveries ranging from 95% to 98% for all examined samples.

Results

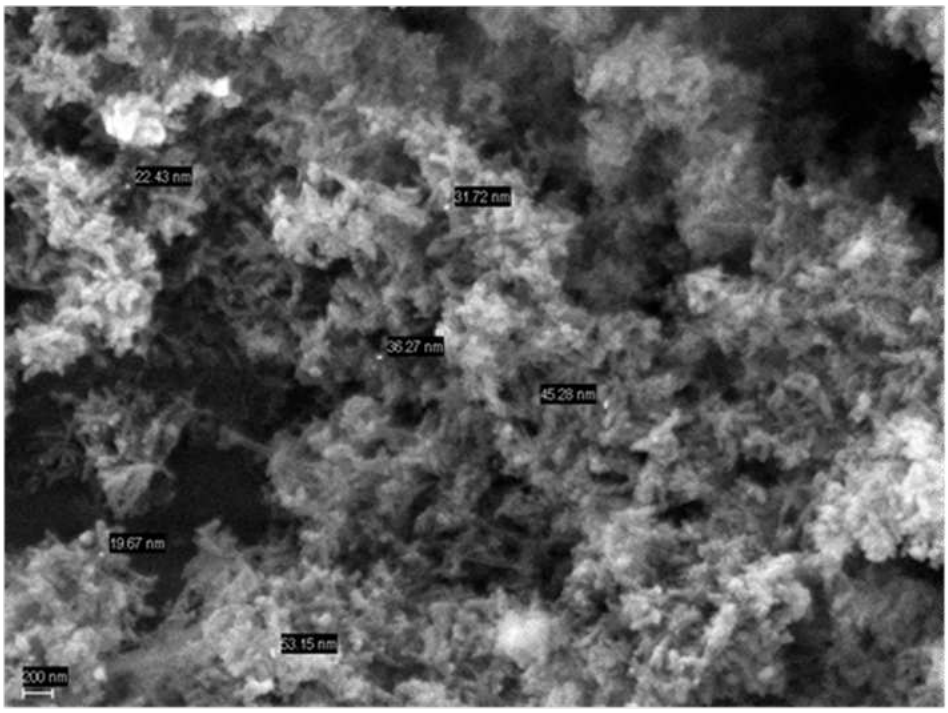
3.1 Characterization of Hydroxyapatites nanoparticles (HANPs))

The analysis of HANPs particles was conducted through various methods. FTIR spectra, using the Nicolate iS5 model, THERMO Electron Scientific Instruments, with 100 mg KBr and 1-2 mg samples, were obtained, revealing spectral data within the range of 500 to 4500 cm^{-1}. Morphological investigations and elemental composition were carried out using a scanning electron microscope (SEM, Carl Zeiss, EVO-18, Research model, Germany) equipped with Energy Dispersive X-ray (EDX) analysis. The SEM examination displayed spherical shapes with clustered distributions with a mean particle diameter of 15-45 nm (Figure 2a, 3a). A recorded EDX spectrum displayed a Ca/P ratio of 1.8 (Figure 2b, 3b) consistent with previous findings reported by Taskin et al. [27] which recorded 1.78. The elemental composition revealed 32% Ca and 17 % P in the HANPs particles.

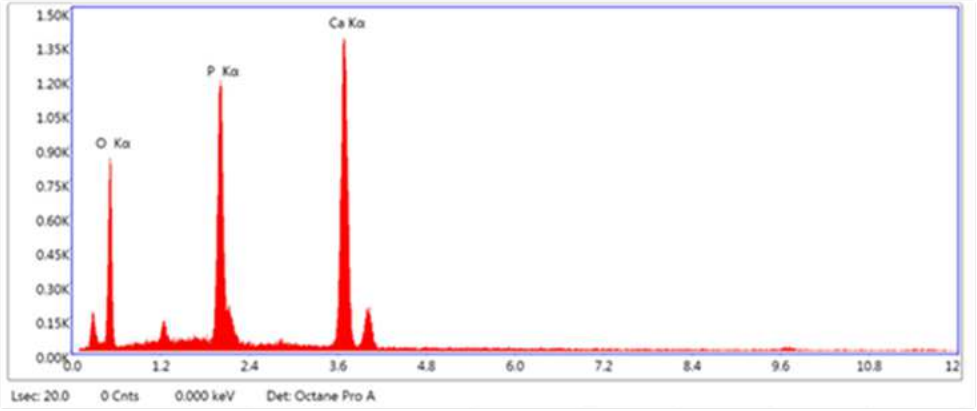
The XRD data were collected between 3 and 90^0 (2θ) at room temperature. Figure 4a, b displays the synthesized HANPs XRD pattern. It was discovered that the hydroxyapatite's typical peak values (25-26, 31-32, 32-33, and 33-34) agreed with previously published (25.5, 31.5, 31.7, 32.1, and 32.5) literature [23,28,29.] The peak pattern indicated that hydroxyapatite was the major mineral phase of the product, whether CMC was added or not. The XRD peak locations were not significantly affected by the presence of the amorphous component, CMC, indicating that no substantial structural changes were produced by the CMC macromolecules and that no new products were formed due to the weak interactions.

The FTIR analysis of calcium phosphate nanoparticles revealed the presence of various functional groups on the nanoparticle surface, including P–O–P bonding, two types of orthophosphate anions (HPO_4^{2-} and PO_4^{3-}), ^{-}OH, and H_2O (figure 5a, b). Additional information on the surface functional groups is illustrated in Figure 4. Transmission at 570 cm^{-1} signifying the stretching of phosphate groups (P-O-P), 887 cm^{-1} (HPO_4^{2-}), 1000 cm^{-1} PO_4^{3-}, 1068 cm^{-1} (P-O), 1400 cm^{-1} (O-H) bending. The findings were in great agreement with the El-Ghany et al.[30]. The values of zeta potential were measured -6.5 ±1.41 mv, -9.6 ±1.00 mv for NP and composite NP, size was in range of 100-300 nm and 100-350 nm for both respective sample.

a



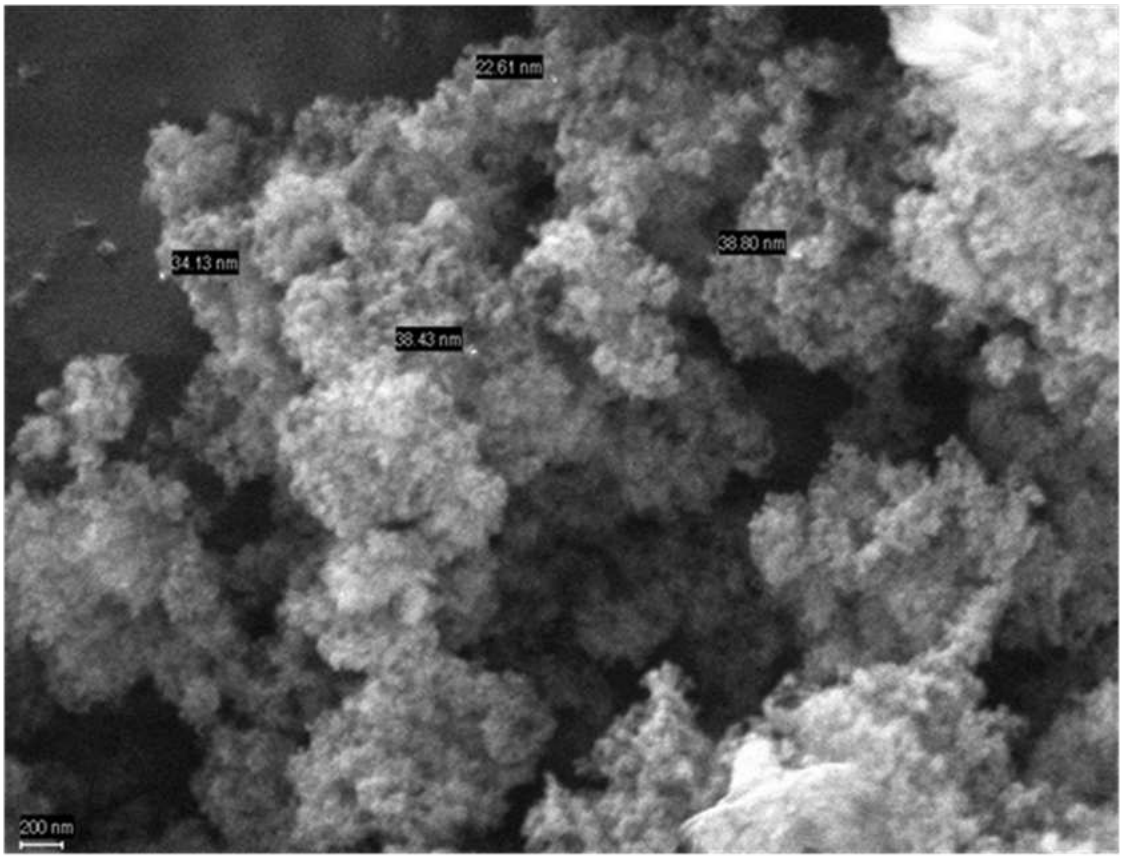
b



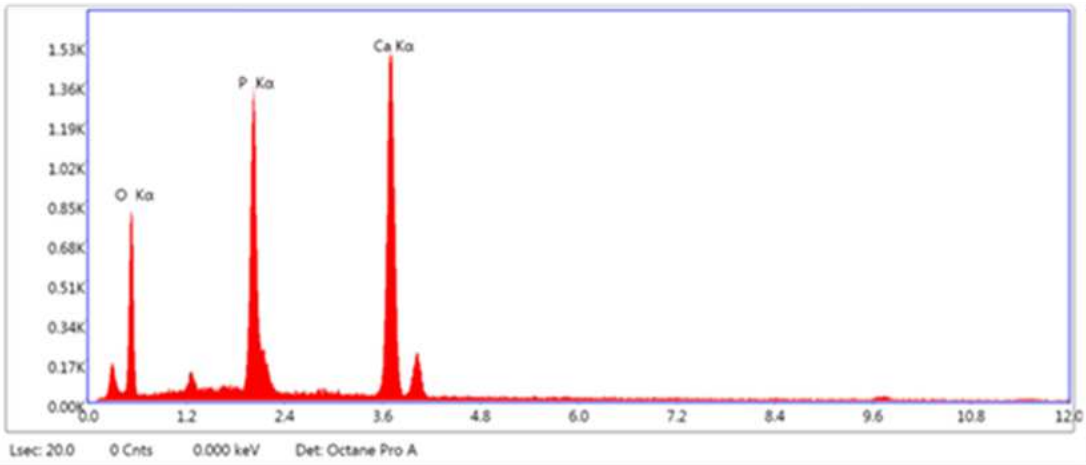
Element	Weight%	Atomic%	Net Int.	Error%	K ratio	Z	A	F
O K	50.64	70.04	258.18	10.98	0.0845	1.0661	0.1567	1.0000
P K	17.69	11.92	445.33	3.79	0.1328	0.9341	0.8457	1.0078
Ca K	32.67	18.04	601.89	2.56	0.2916	0.9192	0.9676	1.004

Figure 2: Figures (a-b) showing SEM image and EDX peak and weight, atomic % of presented elements in HANPs

a



b



Element	Weight%	Atomic%	Net Int.	Error%	K ratio	Z	A	F
O K	49.98	69.50	343.95	10.82	1.0671	0.1543	0.1567	1.0000
P K	16.76	12.04	612.81	3.62	0.9350	0.8457	0.8457	1.0078
CaK	34.26	18.46	839.26	2.43	0.9201	0.9673	0.9676	1.039

Figure 3: Figures (a-b) showing SEM image and EDX peak and weight, atomic % of presented elements in HANPs

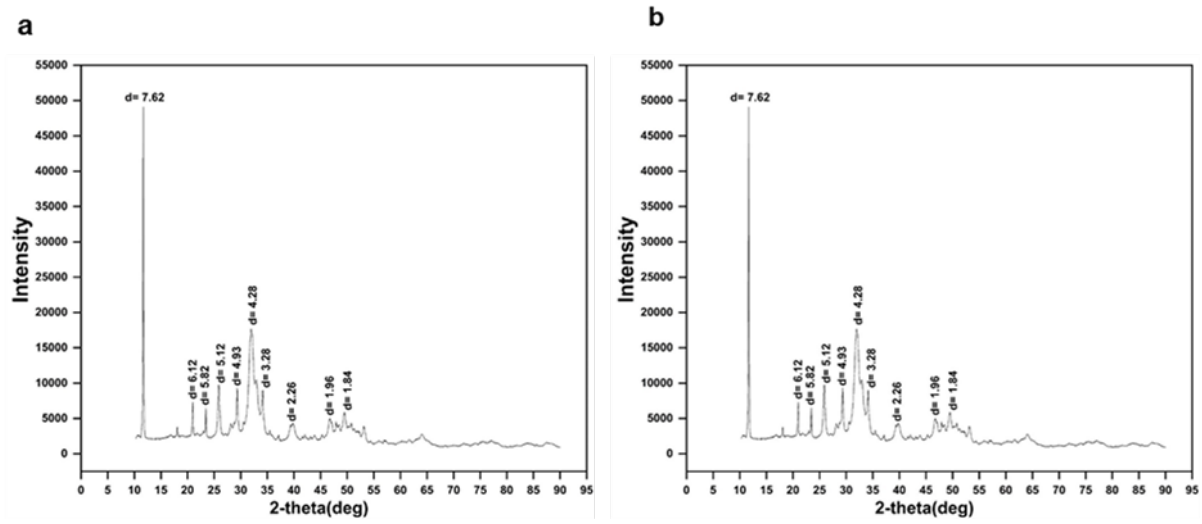


Figure 4: Figures (a-b) showing X-ray diffraction peak of synthesized nanoparticle (HANPs) a- XRD peak of HANPs b- XRD peak of composite HANPs

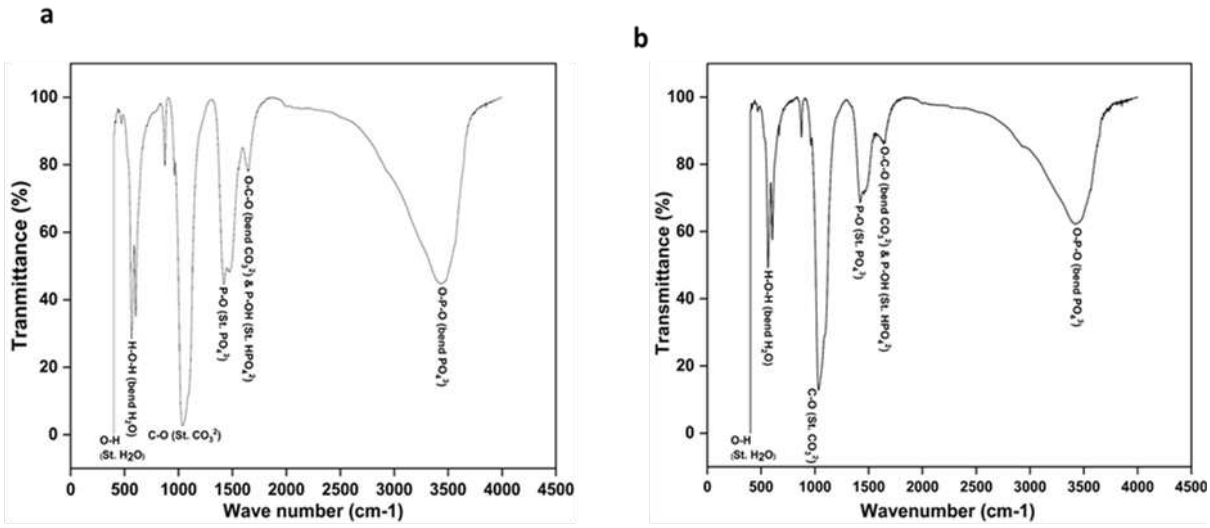


Figure 5: Figures (a-b) Showing FTIR pattern of two synthesized HANPs a-FTIR peak of HANPs b- XRD peak of composite HANPs

3.2 Topsoil Physicochemical Parameters and Element Concentrations

The soil pH levels in Ghazipur (Field 1) and Jaunpur (Field 2) were found within the range of 7.6-8.1 and 8.2-8.4, respectively. The electrical conductivity (EC) values measured were 119 S cm^{-1} for Field 1 and 126 S cm^{-1} for Field 2. The properties are shown in **Table 1.**

Soil of two-time point (during transplantation and at time of harvesting) was taken to know the effect of NP on soil. The results showed that pH was not affected, EC was found to be increased and the soil available P at the time of harvesting was lesser in NP applied block than the conventional fertilizer applied block. Soil enzymes protease, acidic monophosphatase and basic monophosphatase was detected and from the result, it has been proved that there was not any negative effect of HANPs on soil application.

S.No.	Soil parameters	Ghazipur						Jaunpur					
		Ist sampling (during transplantation)			2nd sampling (harvesting)			Ist sampling (during transplantation)			2nd sampling (Harvesting)		
		Control	T1	T2	Control	T1	T2	Control	T1	T2	Control	T1	T2
1	pH	7.74±0.05	7.34±0.05	7.3±0.01	7.8±0.06	7.6±0.01	7.1±0.05	8.2±0.02	8.1±0.01	8.2±0.05	8.4±0.07	8.2±0.02	7.9±0.02
2	EC (µS cm^{-1})	103±4.00	106±2.00	111±9.00	110±3.00	115±7.00	121±6.00	130±6.07	128±2.51	118±2.84	145±5.90	135±2.90	140±6.00
3	Organic carbon (%)	1.18±0.2	1.2±0.1	1.2±0.2	1.19±0.05	1.14±0.06	1.15±0.05	1.49±0.02	1.45±0.05	1.53±0.12	1.62±0.08	1.58±0.03	1.75±0.07
4	ORP	175±0.5	180±1.0	188 ±0.5	190 ±1.0	180±1.5	197± 0.8	186 ±0.5	178±1.0	175 ±0.5	190 ±0.5	190 ±0.5	185 ±0.5
5	Available phosphorus (kg ha^{-1})	87± 3.20	83±1.90	87±3.50	83±1.90	78±2.50	71±1.50	75±5.00	81±4.00	78±2.50	80±4.00	79±2.40	71±6.00
6	Protease (µg tyrosine g^{-1} dw 2 h^{-1})	5.4±0.79	5.5±0.27	5.3±0.55	5.8±0.90	5.1±0.50	5.9±0.50	7.06±1.60	6.8±0.60	8.3±0.20	7.8±0.70	7.2±0.50	8.5±0.70
7	Acidic MP (p-nitrophenol (µg g^{-1} dw h^{-1})	115±5.00	120±3.00	121±1.40	130±2.00	127±1.10	139±1.40	125±1.50	131±3.20	120±4.00	124±0.80	139±4.00	130±1.50
8	AlkalineMP (p-nitrophenol (µg g^{-1} dw h^{-1})	141±2.00	145±2.00	147±4.00	145±4.00	155±3.00	150±1.50	157±4.00	165±2.00	161±0.10	108±1.40	101±4.00	106±2.00
9	P (mg kg^{-1}) P_2O_5	2350±1.0	2510±1.2	2650±1.5	2530±2.00	1930±2.0	2220±1.5	2630±2.00	2580±1.50	2470±1.0	2690±1.0	2000±10.0	2250±1.00
10	Soil As (µg g-1)	17.5±0.03	17.5±0.02	17.2 ±0.02	14.5±0.02	15.0±0.2	15.9±0.3	16.5±0.1	16±0.20	16±0.20	14.0±0.3	15.2±0.20	14.5±0.20

Table.1. Soil physicochemical properties (pH, EC, Organic carbon, available phosphorus, soil enzymes and elemental concentration (P and As) of selected agricultural top soil from study area

3.3 Rice Growth of Two Cultivars Grown in Different Fields

The effect of two different fertilization methods (Foliar sprayed NP (T1) and soil mixed NP (T2) with 100% of the recommended fertilizer dose (RDF) on the growth attributes of two locally used rice varieties (DS and SK) is shown in Figure 6. The growth characteristics of rice plants in the field were analyzed using root and shoot length, biomass, panicle length, number of fertile spikelets, number of grains per spikelet, and 1000 grain weight. Notable increments in root and shoot length were observed in NP-amended block plants compared to the control plants. In Field 1, foliar sprayed plants exhibited greater root length compared to soil-treated NP and control plants. DS variety showed better root growth than SK. While in case of shoot length, the growth pattern was same for both sites. In Field 1, the improvement in T1 for SK and DS was 25% RL, 12% SL and 35% RL, 5% SL, respectively. For T2, the improvement was 3.7% RL, 6.4% SL for SK and 5% RL, 7% SL for DS. In Field 2, T1 showed 4% RL, 5%

SL for SK, 4% RL, 14% SL for DS, and T2 showed 10% RL, 1.4% SL for S.K, 5.8% RL, 8.9% SL for DS (Figure 6 a, b).

Notably, T1 exhibited the highest panicle length in both DS and SK varieties, with a 4.5% increase for DS and 1.8% for SK in Field 1, and an 11% and 8.2% increase in Field 2 for the respective varieties. The number of grains per panicle, 1000-grain weight, and the number of fertile spikelets were improved in the NP treated crops. The number of grains per panicle increased by 4.9% for SK and 6.6% for DS in Field 1 and by 7.1% for SK and 8.4% for DS in Field 2. The 1000-grain weight improved by 5.6% for SK, 9.4% for DS in Field 1, and by 10.6% for SK, and 28% for DS in Field 2. Fertile spikelets increased by 3% for Field 1 and 4% for Field 2 for SK and 9.6% and 5.4% for DS, respectively for the T1(Figure 6 c, d, e, f).

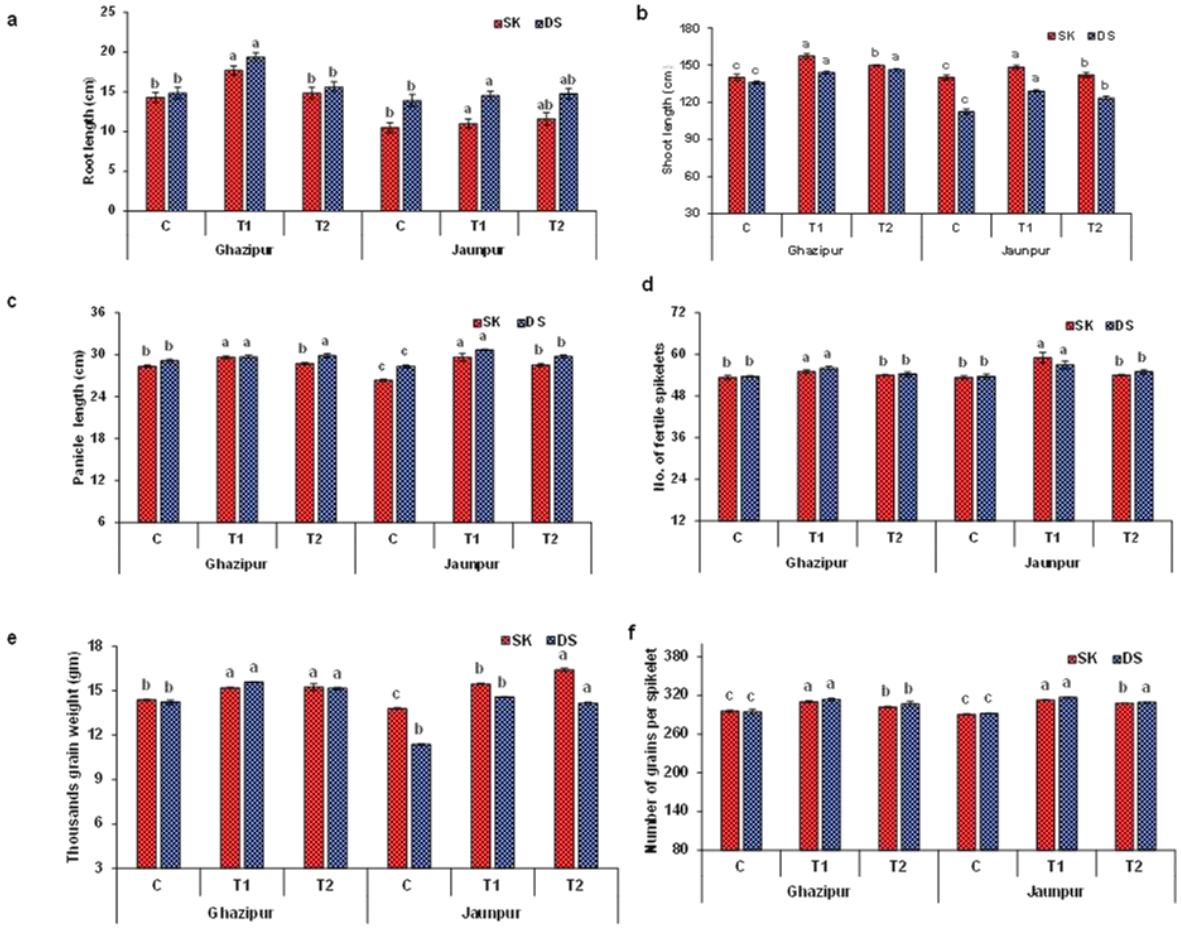


Figure 6: Figure (a-f) showing the morphological appearance, root length (cm), shoot length (cm), panicle length and number of fertile spiklets, thousands grain weight (g), number of grains per spikelet under control and nano P fertilizer application by foliar (T1) and soil application (T2) dose for selected variety (SK, DS) at the respective As contaminated sites (Ghazipur and Jaunpur). Bars represent mean ± SD (n = 3). Different lowercase letters

indicate significant differences among treatments within the same location and variety according to Tukey's multiple comparison test ($p < 0.05$).

3.4 Electrolytic Leakage, Lipid Peroxidation, and Pigment content

Malondialdehyde (MDA), a marker for membrane damage, showed changes in both roots and shoots. In Field 1, SK showed roots MDA reduction by 0.9% in T1 and 18% in T2 and in shoots by 11% in T1 and 16% in T2. Similarly, DS showed variations in roots by -0.9% in T1 and -1.9% in T2 and in shoots by -30% in T1 and -21% in T2. Field 2 also showed a decrease in MDA in both roots and shoots for both varieties in T1 and T2 (Figure 7a, b).

Electrolytic leakage was increased in foliar treated roots but decreased in soil-treated NP treatments. It decreased in shoots for both treatments. In Field 1, for SK, there was a decrease of 39% in roots and 24% in shoots in T2, while DS showed a decrease of 23% in roots and 24% in shoots for T2, and an increase of 8% in roots and decrease of 22% in shoots for T1. In Field 2, SK and DS exhibited different decreases in roots and shoots for both T1 and T2 (Figure 7c, d).

The chlorophyll content of the plant's leaves was notably influenced by HANPs application in both foliar and soil methods for both varieties and in both fields. The chlorophyll content was increased significantly by HANPs delivered through both methods for both varieties in the two selected fields (8a, b, c)

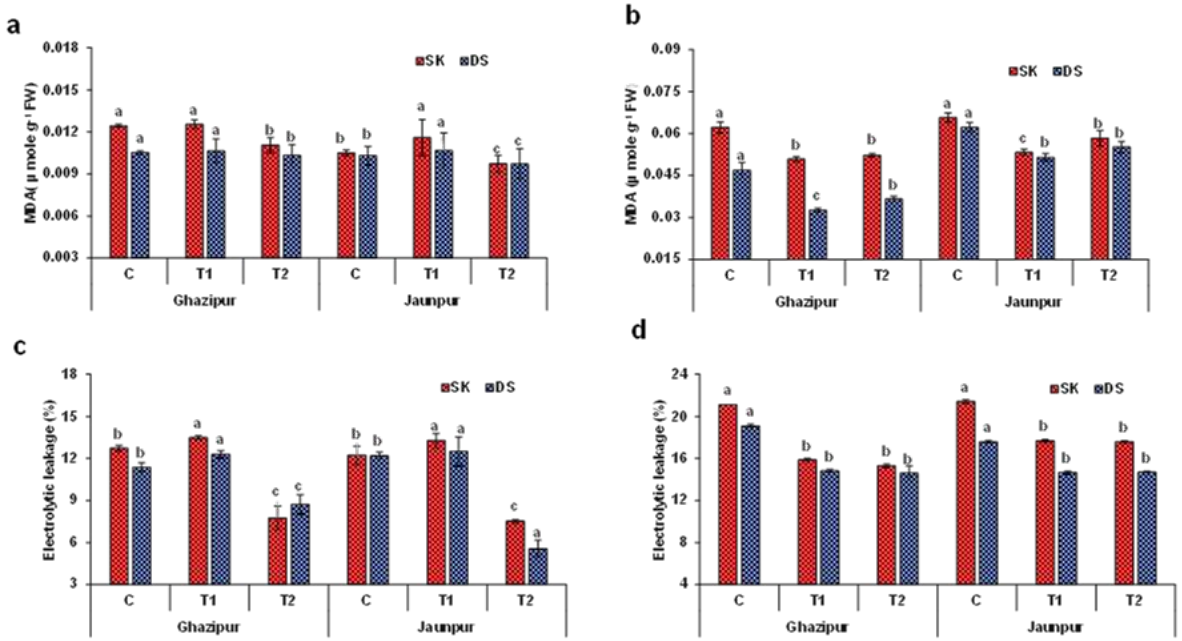


Figure 7: Figure (a-d) showing the physiological response (a-root MDA, b- shoot MDA, c- root electrolytic leakage, d- shoot electrolytic leakage) under control and nano P fertilizer application by foliar (T1) and soil application (T2) dose for selected variety (SK, DS) at the respective As contaminated sites (Ghazipur and Jaunpur). Bars represent mean ± SD (n = 3). Different lowercase letters indicate significant differences among treatments within the same location and variety according to Tukey's multiple comparison test ($p < 0.05$).

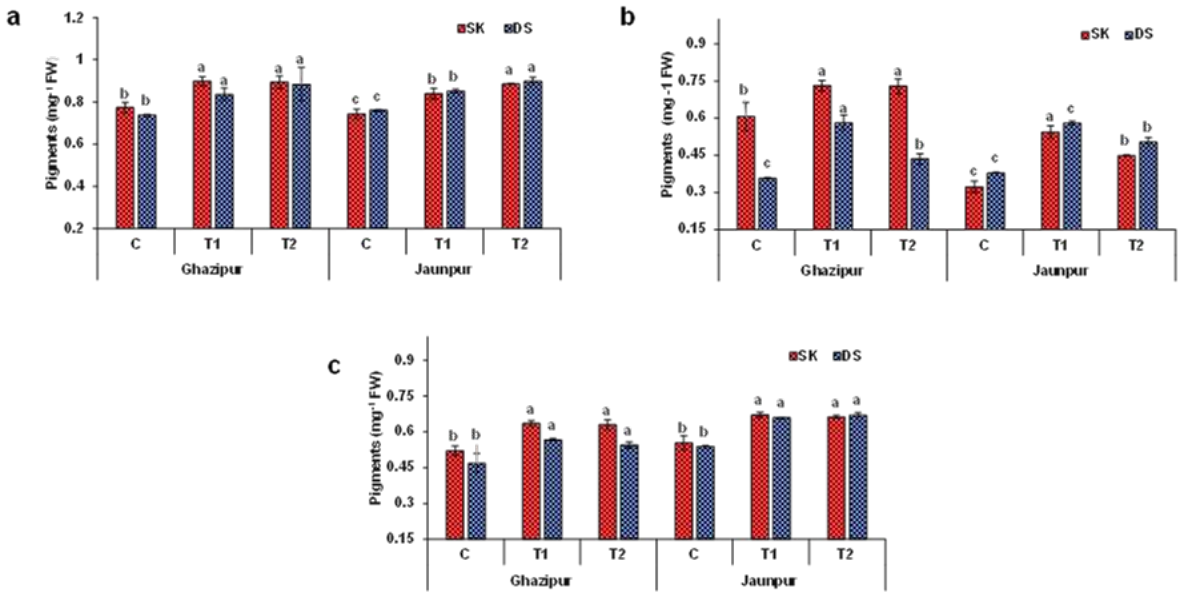


Figure 8: Figure (a-c) showing the physiological response (a-chl a, b-chl b, c- carotenoids) under control and nano P fertilizer application by foliar (T1) and soil application (T2) dose for selected variety (SK, DS) at the respective As contaminated sites (Ghazipur and Jaunpur). Bars represent mean ± SD (n = 3). Different lowercase letters indicate significant differences among treatments within the same location and variety according to Tukey's multiple comparison test ($p < 0.05$).

3.5 Antioxidant Enzyme Activity

The antioxidant enzymes SOD, APX, CAT and GPX showed changes in both treatments compared to the control (Figure 9,10 a-d). Root APX showed a non-significant decrease under T1 for both varieties in both fields, but it increased in T2 by 14% for both varieties in Field 1 and by 2% in Field 2. Shoot APX significantly increased by 71% and 61% for SK and DS, respectively, under T1 in Field 1. Under T2, it increased by 57% and 46% for the respective varieties. In Field 2, there was a non-significant increment of 21% and 14% under T1 for SK

and DS, respectively. For T2, it increased by 29% and 8% for the respective varieties (Figure 9 c, d). Similar trends were observed for GPX. It decreased in the root under T1 for both fields and both varieties but increased in T2, showing increments of 16% and 25% in Field 1 and 20% and 24% in Field 2 for SK and DS, respectively. For the shoot, it increased at Field 1 under T1 (34%, 26%) and T2 (28%, 27%) for the SK and DS, respectively. At Field 2, it increased under T1 (15%, 25% for SK and DS) and T2 (24%, 22% for SK and DS) (Figure 10 a, b). SOD and CAT showed similar patterns, indicating a decrease in root under foliar sprayed NP treatment and an increase under NP-treated soil for both fields and both varieties. Conversely, the shoot showed an increase under both treatments in both fields for both varieties (Figure 9 a, b, 10 c, d).

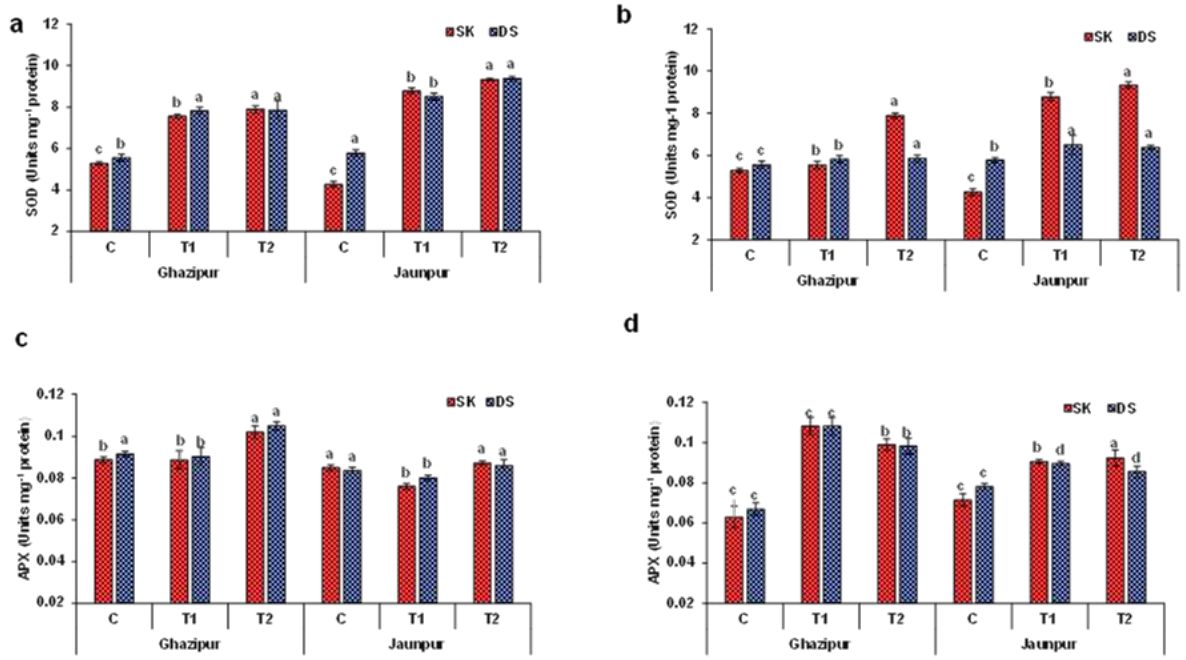


Figure 9: Figure (a-d) showing the biochemical response (a-root SOD, b-shoot SOD, c-root APX, d-shoot APX) under (C), half (P1) and double (P2) phosphors fertilizer dose for selected variety (SK, DS) at the respective As contaminated sites (Ghazipur and Jaunpur). Bars represent mean ± SD (n = 3). Different lowercase letters indicate significant differences among treatments within the same location and variety according to Tukey's multiple comparison test ($p < 0.05$).

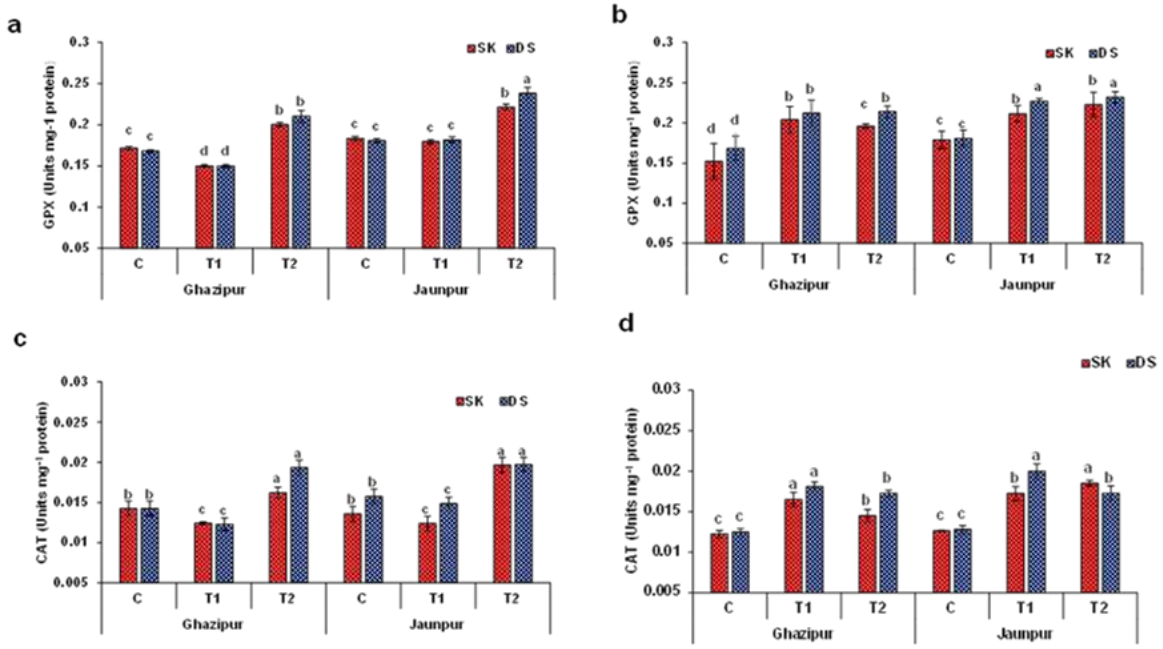


Figure 10: Figure (a-d) showing the biochemical response (a-root GPX, b-shoot GPX, c-root CAT, d-shoot CAT) under control and nano P fertilizer application by foliar (T1) and soil application (T2) dose for selected variety (SK, DS) at the respective As contaminated sites (Ghazipur and Jaunpur). Bars represent mean ± SD (n = 3). Different lowercase letters indicate significant differences among treatments within the same location and variety according to Tukey's multiple comparison test ($p < 0.05$).

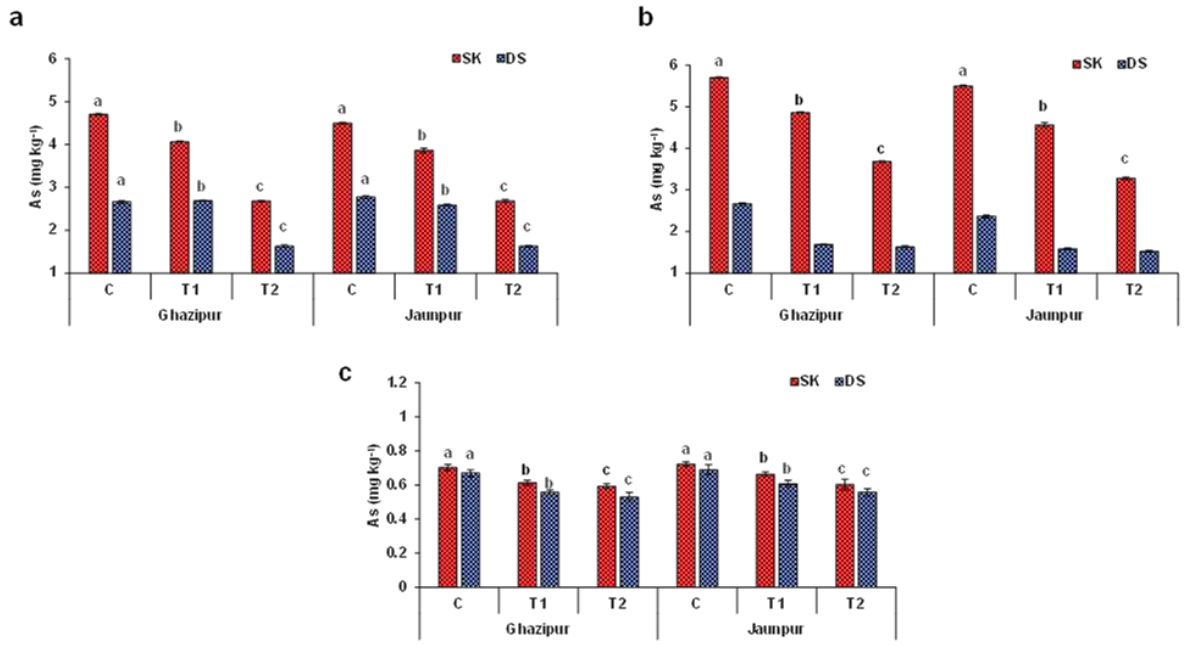
3.6 Arsenic buildup trend in several rice cultivar sections

The analysis of arsenic (As) concentration revealed that the SK cultivar accumulated higher levels of As compared to the DS cultivar. This higher concentration of As was observed in all plant parts, with the order of concentration being root > shoot > grains for both varieties.

The supplementation of nanoparticles had a noticeable impact on reducing As concentration in all plant parts in both cultivated field areas. Specifically, there was a reduction in grain As concentration ranging from 8% to 21% for both fields. In the control fields, the grain As concentration ranged from 0.66 to 0.72 mg kg^{-1} for non-NP treated plants and 0.5 to 0.66 mg kg^{-1} for NP-treated plants, showing a significant reduction.

This significant reduction in As concentrations in grains was consistently observed across all experimental fields, including experimental field 1 (12.5% to 21.0% reduction) and experimental field 2 (8.2% to 18.9% reduction).

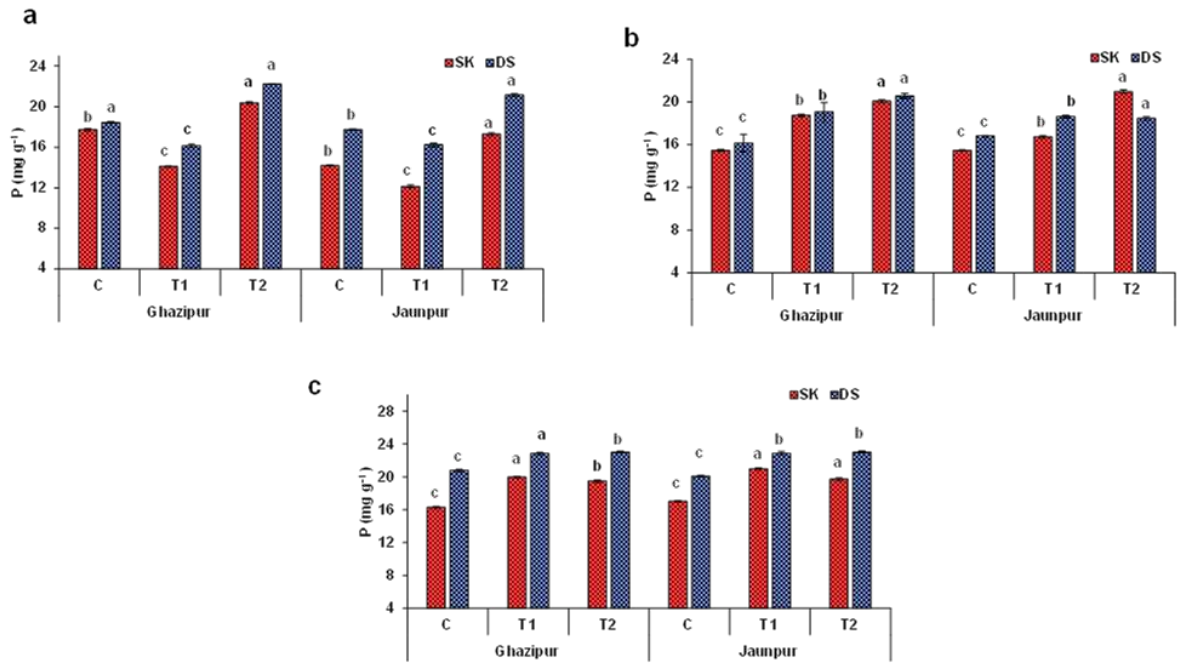
In addition to grains, the reduction in root and shoot As concentration was also noted in plants grown in fields treated with NPs. In fields without NP treatment, plants had higher As concentrations in both roots and shoots. However, plants in fields treated with foliar-sprayed NPs and soil-applied NPs exhibited variable reductions in root and shoot As concentration.



Figures11: Figure (a-c) showing the As accumulation (a- root As concentration, b- shoot As con-centration, c-grain As concentration) under control, half and double dose of P fertilizer for selected variety (DS and SK). Bars represent mean ± SD (n = 3). Different lowercase letters indicate significant differences among treatments within the same location and variety according to Tukey's multiple comparison test ($p < 0.05$).

3.7 Phosphorus accumulation pattern in different parts of rice cultivars

As anticipated, the HANPs treatment raised the rice grains, shoot and root's P content. However, DS T2 (soil treated) at Jaunpur had the highest P content of rice grains (23 mg g^{-1}). The highest accumulation of P was noted in soil treated HANPs for DS and SK for the both fields site T1 also had the greater and significant accumulation of P in root, shoot and grains with respect to control at the both field site (Figure 12a-c)



Figures12: Figure (a-c) showing the P accumulation (a- root P concentration, b- shoot P concentration, c-grain As concentration) under control, half and double dose of P fertilizer for selected variety (DS and SK). Bars represent mean ± SD (n = 3). Different lowercase letters indicate significant differences among treatments within the same location and variety according to Tukey's multiple comparison test ($p < 0.05$).

3.8 Morphological differences and yield enhancement

The results of the morphological analysis indicate a substantial influence of nanofertilizers application on plant development by the both delivered methods, foliar as well as soil application (Table 2). Total yield was increased in both varieties by the application of nano-P fertilizers. The yield was found to be increased in range of 18-20% by the application of NP by using both delivery methods.

		SK Variety			DS Variety		
	Yield	**kg/100ft²**	**kg/hectare**		**kg/100ft²**	**kg/hectare**	
Jaunpur	**Control**	3.38 ±0.31	3637.34±329.71		3.88 ±0.22	4179.84 ±235.78	
	T1	3.90 ±0.05	4197.06 ±51.27	15.39 %	4.59 ±0.38	4944.51 ±413.14	18.30%
	T2	4.06 ±0.04	4374.45 ±46.61	20.25%	4.62 ±0.42	4973.78 ±447.45	19.00%
Ghazipur	**Control**	2.95±0.13	4967.55±141.06		3.38±0.42	3640.78±456.77	
	T1	3.55±0.22	3821±235.78	20.21%	4.11±0.25	4419.23±270.33	21.38%
	T2	3.57±0.38	3844±412.38	20.91%	4.07±0.46	4381.34±493.73	20.34%

Table.2. Yield difference in control and NP amended plant

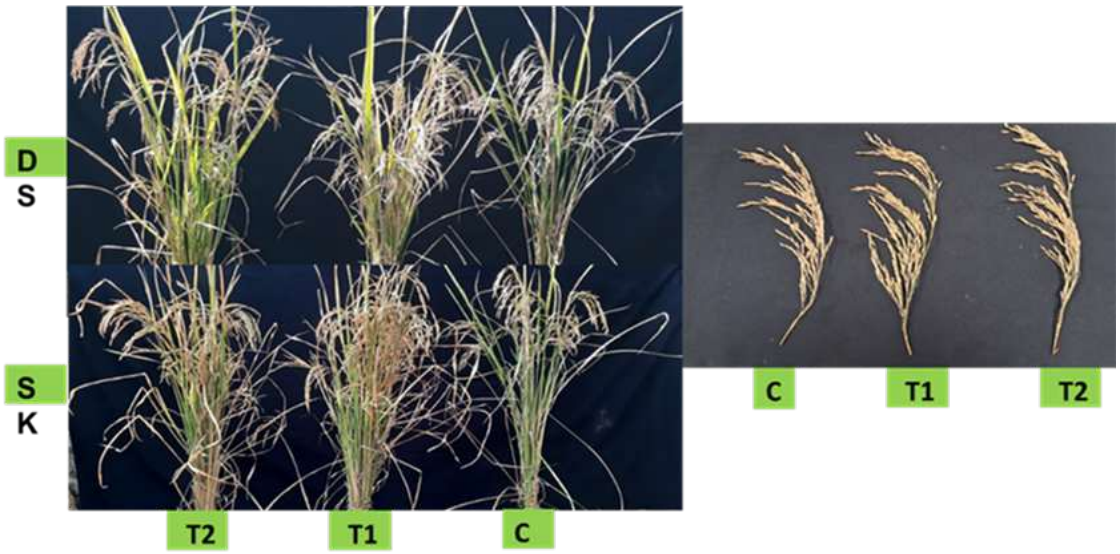


Figure 13: Morphological difference of two selected genotypes under nano-P fertilizer dose in respect to control

4 Discussion

The investigation of the two different fertilization methods, namely foliar sprayed NP (T1) and soil mixed NP (T2) at 100% of the recommended fertilizer dose (RDF) on the growth characteristics of the selected rice varieties exhibited notable outcomes. In Figure (2), T1 showed a significant impact on the panicle length for both DS and SK varieties, displaying a 4.5% increase for DS and 1.8% for SK in Field 1, and an 11% and 8.2% increase in Field 2, respectively. Furthermore, several growth attributes were positively influenced by the NP treatments[39].Apatite nanoparticles were found to be stable and precipitate-free for several months in a suspension of carboxymethyl cellulose (CMC) by Liu and Lal [9]. An experiment by Liu and Lal [9] demonstrated that conventional apatite cannot blend with the soil solution or traverse soil columns. In contrast, particles of nanosized apatite granules showed increased mobility in the soil, as they stayed on the soil column[40]. This suggests that nanosized apatite granules may be more advantageous than their conventional counterparts in delivering phosphorus to plant roots. Bala et al. [31] explored the positive impact of hydroxyapatite nanorods on pea germination and growth. Their findings indicated that the application of hydroxyapatite nanorods resulted in enhanced rates of plant growth and germination.

In the present study also, there was significant improvement in various growth and yield parameters analyzed in response to HANPs treatments, with more pronounced effect being in grains per panicle, 1000-grain weight and number of fertile spikelets. The outcomes of a foliar application of nano-calcium phosphate (NCaP) revealed significant improvements[41]. NCaP demonstrated a substantial increase in both shoot and root dry weights, enhanced nutrient content in the shoot and root, improved yield components, and elevated nutrient concentration and crude protein percentage in snap bean (*Phaseolus vulgaris L.*) pods, as compared to traditional P applications. The most notable enhancements were observed when a 20% NCaP soil application was combined with a 5% NCaP foliar application. Based on these findings, the study recommends considering NCaP as an alternative P source to alleviate the adverse effects associated with traditional sources [30]. In this study, electrolytic leakage and lipid peroxidation, indicating membrane permeability and cellular damage, respectively, exhibited varied trends based on the NP treatments. Electrolytic leakage increased in foliar treated roots but decreased in soil-treated NP treatments[42]. There was a noticeable decrease in MDA (a marker for membrane damage) in both roots and shoots for T1 and T2 in Field 2 for both varieties. The optimal concentration of nanoparticles plays a crucial role in activating the antioxidant defence system[43]. This activation, in turn, triggers the plant defense system and helps maintain reactive oxygen species (ROS) at an ideal level to convey stress signals [32].

The chlorophyll content, an indicator of photosynthetic capability, showed a considerable increase after NP application in both foliar and soil methods for both varieties and in both fields. Notably, the chlorophyll content was significantly enhanced by NP delivered through both methods. In a pot experiment Li and Huang et al[33]. investigated the impact of hydroxyapatites nanoparticles (HANPs) on various factors in Pakchoi (*Brassica chinensis L.*) grown in Cd contaminated soil. The study assessed biomass, cadmium uptake, chlorophyll content, vitamin C, MDA, and activities of antioxidant enzymes such as SOD, CAT, and peroxidase (POD). The results revealed that the use of hydroxyapatite nanoparticles (HANPs) led to a decrease in MDA levels and an increase in the concentrations of vitamin C and chlorophyll in the shoot portion[43]. Additionally, the application of HANPs to contaminated soils resulted in heightened activity of SOD, CAT, and POD. Like the calcium concentration observed in cell, nanoparticles have been found to stimulate the production of nitric oxide (NO) [44]. Nitric oxide functions as a stress messenger molecule, triggering stress-related genes that activate the immune system. This activation, in turn, results in stress tolerance[34].

In our study antioxidant enzyme activities (APX, GPX, CAT, and SOD) also displayed variations in response to the HANPs treatments. These enzymes showed notable changes in both root and shoot structures, particularly under T2, signifying the influence of nano-phosphorus on the antioxidative defense system of rice plants which is in strong agreement with the previous findings[45].

Chen et al. [34]successfully remediated heavy metals, including cadmium, zinc, copper, and lead, in contaminated soil by utilizing a biochar blend with hydroxyapatite/calcium silicate hydrates. According to their study, the concentration of heavy metals in spinach *(Ipomoea aquatica forsk.*) decreased by approximately 73%. In our study, the use of HANPs resulted in a decline in As accumulation in both vegetative tissue and grains compared to the control, with the most substantial reduction being 27% in grain As accumulation. This observation aligns with the findings of Gu et al. [35], who examined the impact of hydroxyapatite biochar zeolite on As and Cd species in a paddy field. Their findings indicated that the application of this compound led to a reduction in the concentration of soluble cadmium and As in the soil. Moreover, there was a significant decrease in the concentration of these elements in rice. As per Jin et al.[37] the application of HANPs at a concentration of 5 g kg^{-1} resulted in the immobilization of lead in contaminated soil and promoted the growth of ryegrass. In a paddy field study, Gu et al [35] investigated the influence of hydroxyapatite, biochar, and zeolite on As and Cd species. They reported a significant reduction in the concentrations of soluble As and Cd in both rice and soil following the application of these compounds. Hydroxyapatite, a calcium phosphate biomaterial, holds promise for addressing soil, water, and air contamination. Its unique structure and exceptional properties, including high adsorption capacity, elevated ion exchange capacity, and satisfactory stability, make it a valuable tool for environmental treatment [36].

This detailed analysis highlights the impact of NP supplementation in reducing As concentrations in different plant parts across various field conditions. The reductions observed in grain, root, and shoot As concentrations indicate the potential of NPs to mitigate As accumulation in crops[46].

Consent to Publish declaration: Not applicable

Consent to Participate declaration: Not applicable

Ethics declaration: Not applicable

Ethics and Consent to Participate: All plant materials used in this study were commercially procured from local markets and included commonly cultivated varieties, as well as plant materials previously reported in our earlier published study[47]. The collection and use of plant materials complied with relevant institutional and national guidelines. No specific permissions or licenses were required as no wild, endangered, or protected species were involved

Clinical trial number: Not applicable

Declaration of competing interest: The authors declare that they have no financial or personal relationships that could have influenced the work reported in this paper.

Data availability: All data generated or analyzed during this study are included in this paper.

Funding Declaration: Kavita Shukla is thankful to CSIR for Junior Research Fellowship (09/013(0818)/2018-EMR-I). Sudhakar Srivastava is thankful to Institute of Eminence, Banaras Hindu University for the research grant (Scheme No. 6031).

References

1. Irfan, M., Abbas, M., Shah, J. A., & Memon, M. Y. (2018). Internal and external phosphorus requirements for optimum grain yield are associated with P-utilization efficiency of wheat cultivars. Communications in Soil Science and Plant Analysis, 49(22), 2843-2853. https://doi.org/10.1080/00103624.2018.1546872

2. Wissuwa, M. (2003). How do plants achieve tolerance to phosphorus deficiency? Small causes with big effects. *Plant Physiology, 133*(4), 1947-1958. https://doi.org/10.1104/pp.103.027350

3. Srivastava, S., Upadhyay, M. K., Srivastava, A. K., Abdelrahman, M., Suprasanna, P., Tran, L. S. P. (2018). Cellular and subcellular phosphate transport machinery in plants. *International Journal of Molecular Sciences, 19*(7), 1914. https://doi.org/10.3390/ijms19071914

4. Nussaume, L., Kanno, S., Javot, H., Marin, E., Pochon, N., Ayadi, A., Thibaut, M. C. (2011). Phosphate import in plants: focus on the PHT1 transporters. *Frontiers in Plant Science, 2*, 83. https://doi.org/10.3389/fpls.2011.00083

5. Awasthi, S., Chauhan, R., Dwivedi, S., Srivastava, S., Srivastava, S., Tripathi, R.D. (2018). A consortium of alga (Chlorella vulgaris) and bacterium (Pseudomonas putida) for

amelioration of As toxicity in rice: A promising and feasible approach. *Environmental and Experimental Botany, 150*, 115-126. https://doi.org/10.1016/j.envexpbot.2018.03.018

6. Upadhyay, M. K., Shukla, A., Yadav, P., & Srivastava, S. (2019). A review of arsenic in crops, vegetables, animals, and food products. *Food Chemistry, 276*, 608-618. https://doi.org/10.1016/j.foodchem.2018.10.066Suriyagoda, L. D., Dittert, K., Lambers, H. (2018). As in Rice soils and potential agronomic mitigation strategies to reduce As bioavailability: a review. *Pedosphere, 28*(3), 363-382. https://doi.org/10.1016/S1002-0160(18)60007-4

7. Suriyagoda, L. D., Dittert, K., & Lambers, H. (2018). Arsenic in rice soils and potential agronomic mitigation strategies to reduce arsenic bioavailability: A review. *Pedosphere*, *28*(3), 363–382. https://doi.org/10.1016/S1002-0160(17)60494-6

8. Zhao, F. J., McGrath, S. P., Meharg, A. A. (2010). As as a food chain contaminant: mechanisms of plant uptake and metabolism and mitigation strategies. *Annual Review of Plant Biology, 61*, 535-559. https://doi.org/10.1146/annurev-arplant-042809-112152

9. Liu, R., & Lal, R. (2014). Synthetic apatite nanoparticles as a phosphorus fertilizer for soy-bean (Glycine max). *Scientific Reports, 4*(1), 5686. https://doi.org/10.1038/srep05686

10. Reynolds, C. S., Davies, P. S. (2001). Sources and bioavailability of phosphorus fractions in freshwaters: a British perspective. *Biological Reviews, 76*(1), 27-64. https://doi.org/10.1017/S1464793101005696

11. Yang, Y., Hu, H., Fu, Q., Zhu, J., Zhang, X., Xi, R. (2020). Phosphorus regulates As uptake by rice via releasing As into soil pore water and sequestrating it on Fe plaque. *Science of the Total Environment, 738*, 139869. https://doi.org/10.1016/j.scitotenv.2020.139869

12. Janmohammadi, M., Amanzadeh, T., Sabaghnia, N., & Dashti, S. (2016). Impact of foliar application of nano micronutrient fertilizers and titanium dioxide nanoparticles on the growth and yield components of barley under supplemental irrigation. *Acta Agriculturae Slovenica, 107*(2), 265-276. https://doi.org/10.14720/aas.2016.107.2.12

13. Liu, H., Shao, B., Long, X., Yao, Y., Meng, Q. (2016). Foliar penetration enhanced by bio-surfactant rhamnolipid. *Colloids and Surfaces A: Physicochemical and Engineering Aspects, 145*, 548-554. https://doi.org/10.1016/j.colsurfa.2016.03.025

14. Walkley, A., Black, I. A. (1934). An examination of the Degtjareff method for determining soil organic matter, and a proposed modification of the chromic acid titration method. *Soil Science, 37*(1), 29-38. https://doi.org/10.1097/00010694-193401000-00003

15. Tabatabai, M. A., Bremner, J. M. (1969). Use of p-nitrophenyl phosphate for assay of soil phosphatase activity. *Soil Biology and Biochemistry, 1*, 301-307. https://doi.org/10.1016/0038-0717(69)90021-8

16. Ladd, J. N., & Butler, J. H. A. (1972). Short-term assays of soil proteolytic enzyme activities using proteins and dipeptide derivatives as substrates. *Soil Biology and Biochemistry, 4*, 19-30. https://doi.org/10.1016/0038-0717(72)90038-7

17. Khanam, N., Mahmood, K., Hossain, M.S., Ali, M.A., Ahsan, N. (2022).

18. Arnon, D. I. (1949). Copper enzymes in isolated chloroplasts. Polyphenol oxidase in Beta vulgaris. *Plant Physiology, 24*(1), 1. https://doi.org/10.1104/pp.24.1.1

19. Heath, R. L., Packer, L. (1968). Photoperoxidation in isolated chloroplasts: I. Kinetics and stoichiometry of fatty acid peroxidation. *Archives of Biochemistry and Biophysics, 125*, 189-198. https://doi.org/10.1016/0003-9861(68)90028-9

20. Dionisio-Sese, M. L., Tobita, S. (1998). Antioxidant responses of rice seedlings to salinity stress. *Plant Science, 135*, 1-9. https://doi.org/10.1016/S0168-9452(98)00108-6

21. Shukla, S. K., Sharma, L., Jaiswal, V. P., & Pathak, A. D. (2023). Interaction of plant growth-promoting rhizobacteria with sugarcane plants for alleviating abiotic stresses and improving crop yields. In *Agro-industrial Perspectives on Sugarcane Production under Environmental Stress* (pp. 123-137). Singapore: Springer Nature Singapore.

22. Bradford, M. M. (1976). A rapid and sensitive method for the quantitation of microgram quantities of protein utilizing the principle of protein-dye binding. *Analytical Biochemistry, 72*, 248–254. https://doi.org/10.1016/0003-2697(76)90527-3

23. Beyer, W. F., & Fridovich, I. (1987). Assaying for superoxide dismutase activity: Some large consequences of minor changes in conditions. Analytical Biochemistry, 161(2), 559-566. https://doi.org/10.1016/0003-2697(87)90489-1

24. Nakano, Y., & Asada, K. (1981). Hydrogen peroxide is scavenged by ascorbate-specific peroxidase in spinach chloroplasts. Plant and Cell Physiology, 22(5), 867-880. https://doi.org/10.1093/oxfordjournals.pcp.a076232Hemeda, H. M., Klein, B. P. (1990). Effects of naturally occurring antioxidants on peroxidase activity of vegetable extracts. *Journal of Food Science, 55*, 184-185. https://doi.org/10.1111/j.1365-2621.1990.tb04576.x

25. Aebi, H. (1974). Catalase. In *Methods of Enzymatic Analysis*. Academic Press, pp. 673-684. https://doi.org/10.1016/S0955-2863(03)00030-5

26. Khanam, R., Kulsum, P. G. P. S., Debnath, S., Roychowdhury, T., & Mandal, B. (2023). Impact of soil amendment regimes on arsenic exposure to human through rice: Risk assessment and prediction for remediation. Exposure and Health, 15(2), 355-371

27. Taskin, H., Gunes, A. (2023). Synthetic nano-hydroxyapatite as an alternative phosphorus source for wheat grown under field conditions. *Journal of Plant Nutrition*, 1-14. https://doi.org/10.1080/01904167.2023.2202322

28. Chen, Z., Liu, Y., Mao, L., Gong, L., Sun, W., Feng, L. (2018). Effect of cation doping on the structure of hydroxyapatite and the mechanism of defluoridation. *Ceramics International, 44*(6), 6002-6009. https://doi.org/10.1016/j.ceramint.2018.01.039

29. Thanh, D. N., Novák, P., Vejpravova, J., Vu, H. N., Lederer, J., Munshi, T. (2018). Removal of copper and nickel from water using nanocomposite of magnetic hydroxyapatite nanorods. *Journal of Magnetism and Magnetic Materials, 456*, 451-460. https://doi.org/10.1016/j.jmmm.2018.01.040

30. El-Ghany, M. F. A., El-Kherbawy, M. I., Abdel-Aal, Y. A., El-Dek, S. I., Abd El-Baky, T. (2021). Comparative study between traditional and nano calcium phosphate fertilizers on growth and production of snap bean (Phaseolus vulgaris L.) plants. *Nanomaterials, 11*(11), 2913. https://doi.org/10.3390/nano11112913

31. Bala, N., Dey, A., Das, S., Basu, R., Nandy, P. (2014). Effect of hydroxyapatite nanorod on chickpea (Cicer arietinum) plant growth and its possible use as nano-fertilizer. *Iranian Journal of Plant Physiology, 4*(3), 1061-1069. https://doi.org/10.22059/ijpp.2014.53622

32. Syu, Y. Y., Hung, J. H., Chen, J. C., & Chuang, H. W. (2014). Impacts of size and shape of silver nanoparticles on Arabidopsis plant growth and gene expression. *Plant Physiology and Biochemistry, 83*, 57–64. https://doi.org/10.1016/j.plaphy.2014.07.010

33. Li, Z., Huang, J. (2014). Effects of nanoparticle hydroxyapatite on growth and antioxidant system in pakchoi (Brassica chinensis L.) from cadmium-contaminated soil. Journal of Nanomaterials, 2014(1), 470962. https://doi.org/10.1155/2014/470962

34. Chen, H., Yuan, X., Xiong, T., Jiang, L., Wang, H., Wu, Z. (2020). Biochar facilitated hydroxyapatite/calcium silicate hydrate for remediation of heavy metals contaminated soils. *Water, Air, & Soil Pollution, 231*(2), 66. https://doi.org/10.1007/s11270-020-04500-w

35. Gu, J. F., Zhou, H., Yang, W. T., Peng, P. Q., Zhang, P., Zeng, M., Liao, B. H. (2018). Effects of an additive (hydroxyapatite–biochar–zeolite) on the chemical speciation of Cd and As in paddy soils and their accumulation and translocation in rice plants. *Environmental Science and Pollution Research, 25*, 8608-8619. https://doi.org/10.1007/s11356-018-1357-6

36. Jin, Y., Liu, W., Li, X. L., Shen, S. G., Liang, S. X., Liu, C., & Shan, L. (2016). Nano-hydroxyapatite immobilized lead and enhanced plant growth of ryegrass in a contaminated soil. Ecological Engineering, 95, 25-29. https://doi.org/10.1016/j.ecoleng.2016.06.071

37. Ibrahim, M., Labaki, M., Giraudon, J. M., Lamonier, J. F. (2020). Hydroxyapatite, a multifunctional material for air, water and soil pollution control: A review. Journal of Hazardous Materials, 383, 121139.https://doi.org/10.1016/j.jhazmat.2019.121139

38. Kaur, S., Kumari, A., Sharma, N., Pandey, A. K., & Garg, M. (2022). Physiological and molecular response of colored wheat seedlings against phosphate deficiency is linked to accumulation of distinct anthocyanins. Plant Physiology and Biochemistry, 170, 338-349.

39. Jiang, M., Dong, C., Bian, W., Zhang, W., & Wang, Y. (2024). Effects of different fertilization practices on maize yield, soil nutrients, soil moisture, and water use efficiency in northern China based on a meta-analysis. Scientific reports, 14(1), 6480.

40. Dhiman, V. K., Dhiman, V. K., Rana, G., Kumar, R., Singh, D., Chauhan, A., & Ghotekar, S. (2025). Recent advances in phosphorus nano-fertilizers: Impacts on crop productivity and soil sustainability. Physiological and Molecular Plant Pathology, 102885. https://doi.org/10.1016/j.pmpp.2025.102885

41. Shabiya, A., Bhat, M. A., Singh, P., Hassan, S., & Hussain, N. (2025). Nanofertilizers: Mechanisms, efficacy, and implications for sustainable agriculture. In Agricultural Nutrient Pollution and Climate Change: Challenges and Opportunities (pp. 311-353). Cham: Springer Nature Switzerland.

42. Kang, M., Liu, Y., Weng, Y., Wang, H., & Bai, X. (2024). A critical review on the toxicity regulation and ecological risks of zinc oxide nanoparticles to plants. Environmental Science: Nano, 11(1), 14-35.

43. Farooq, M. A., Hannan, F., Islam, F., Ayyaz, A., Zhang, N., Chen, W., ... & Zhou, W. (2022). The potential of nanomaterials for sustainable modern agriculture: present findings and future perspectives. Environmental Science: Nano, 9(6), 1926-1951.

44. Kumari, A., Kumar, A., Seth, A., Guleria, I., Arya, V., & Shahi, S. K. (2024). Nanotechnology Intervention for Sustainable Agriculture: Challenges and Possibilities. Nanotechnology: Agriculture, Environment and Health, 1-51.

45. Andrabi, S. M., Sharma, N. S., Karan, A., Shahriar, S. S., Cordon, B., Ma, B., & Xie, J. (2023). Nitric oxide: physiological functions, delivery, and biomedical applications. Advanced Science, 10(30), 2303259.

46. Najm, S. H., & Al-Juthery, H. W. A. (2023). Effect of Phosphorous, Potassium Nano-Fertilizers and Spraying of (Sepehr 4) Nano-Fertilizer and Carbon Nanotubes on the Growth and Yield of Rice (Oryza sativa L.). In IOP Conference Series: Earth and Environmental Science (Vol. 1259, No. 1, p. 012016). IOP Publishing.

47. Shukla, K., Singh, S. & Srivastava, S. (2024) Evaluation of Response of Rice Varieties Differing in Phosphorus Use Efficiency Under Arsenic Stress. J Plant Growth Regul 43, 4653–4666 (2024). https://doi.org/10.1007/s00344-024-11423-7